An Automated Approach for $q\bar{q} \to b\bar{b}b\bar{b}$ at Next-to-Leading Order QCD

T. Reiter*

12 February 2009

Abstract

The search for the Higgs boson and for physics beyond the Standard Model are the major motivations behind the LHC experiment. In many scenarios the success of the experiment depends on the knowledge of signal and background event rates at least at one-loop precision. We present the approach of the GOLEM collaboration to build a highly automated framework for the calculation of matrix elements at the one-loop level, which is based on the evaluation of Feynman diagrams. Part of this effort is an open-source library for the numerical evaluation of tensor integrals. As an application, some results for the process $pp \to b\bar{b}b\bar{b}$ calculated with this method are presented.

PACS 12.38.Bx, 13.85.Hd

Keywords perturbative QCD, LHC phenomenology, radiative corrections

1 Introduction

The Standard Model of Particle Physics has been tested by previous collider experiments to a very high precision [1]. Despite its great success, many fundamental questions such as the nature of dark matter cannot be addressed within the Standard Model. Two main goals of the next collider experiment, the LHC, are therefore the discovery (or exclusion) of a Standard Model Higgs boson and the measurement of any new particles accessible by the collider energy [2]. Due to the purely hadronic initial state of the collisions one expects the interactions mainly to be governed by QCD. A precise understanding of both the signal and the background will be crucial for most Higgs discovery channels and for the discrimination of different scenarios beyond the Standard Model. For many processes a Leading Order

*Nikhef, Science Park 105, 1098 XG Amsterdam, The Netherlands

(LO) approximation will not suffice and has to be amended by higher order corrections.

The calculation of matrix elements at LO has become an automated routine for which many computer programs are available [4, 5, 6, 7, 8, 9]. Next to Leading Order (NLO) calculations, however, have never reached this level of automation. Especially in the case of many particle final states (≥ 3 final state particle) automatisation is not straightforward as one easily hits the limits of current computer technology. A full NLO calculation in QCD consists of a $2 \rightarrow n$ particle tree-level contribution (LO), the real emission of an extra parton ($2 \rightarrow n + 1$, tree-level) and virtual corrections ($2 \rightarrow n$, one-loop diagrams). Both real and virtual corrections can contain infrared divergences which only cancel in the sum of both contributions. These divergences can be dealt with by subtraction methods [10, 11] which have also become available as automated implementations [12, 13, 14, 15]. The only missing ingredient for a full automation of NLO calculations are the virtual corrections. Although many different methods have been proposed [16, 17, 19, 20, 21, 22, 23, 24] no fully automated implementation has been made available yet. The very limited number of results found in the literature for processes with four final state particles [25, 26, 27, 28, 29, 30] underlines the importance of automatisation in the context of one-loop calculations.

The GOLEM collaboration focuses on the development of such an automatised tool for one-loop matrix element calculations[1]. We have applied the GOLEM method to calculate the QCD one-loop corrections of the process $u\bar{u} \rightarrow b\bar{b}b\bar{b}$, which is a subprocess of $pp \rightarrow b\bar{b}b\bar{b}$. This process is a particular important background in MSSM Higgs searches at large values of $\tan\beta$, where one of the Higgs bosons decays predominantly into $b\bar{b}$ pairs.

2   The GOLEM Approach

Our approach is based on the calculation of Feynman diagrams. We generate the diagrams and their corresponding algebraic expressions using QGraf [31] and project them on a colour and helicity basis. The integration over the momentum of the virtual particle introduces tensor integrals of the form

$$I_N^{n;\mu_1,\ldots,\mu_r} = \int \frac{\mathrm{d}^n k}{i\pi^{n/2}} \frac{k^{\mu_1} \cdots k^{\mu_r}}{\prod_{j=1}^N \left[(k + r_j)^2 - m_j^2 + i\delta\right]} \tag{1}$$

These integrals are reduced to a basis of scalar integrals by the method described in [32, 33]; we use two independent implementations where

   a) the tensor reduction is carried out on a symbolical level and the amplitude is represented in terms of Mandelstam variables, Levi-Civita

---

[1]GOLEM stands for General One Loop Evaluator for Matrix elements

tensors and the commonly used standard basis of scalar one-loop integrals

$$\mathcal{M}_{\{\lambda\},c} = C_{\text{box}} I_4^n + C_{\text{tri}} I_3^n + C_{\text{bub}} I_2^n + C_{\text{tad}} I_1^n.$$

The algebraic reduction and further simplifications are achieved using `Form` [34] and Maple.

b) a form factor representation is introduced for the tensor integrals and the tensor reduction is delayed until the numerical evaluation. The form factors are implemented in the Fortran library `golem95` which is described in [35]. The amplitude is represented in terms of Mandelstam variables, spinor bi-products $\bar{u}(p_i)(1 \pm \gamma_5)u(p_j)$ and an extended basis of one-loop integrals that allows for Feynman parameters in the numerator.

In both strategies, Gram determinants in the denominator are either avoided or to some extent cancelled explicitly on the symbolical level, thus resulting in a numerically stable implementation of the matrix element.

The results presented below have been obtained with implementation b) in which the user starts from a very minimal process description. All necessary files are generated by a `Python` script. The matrix element is obtained as a set of `Fortran90` files which are compiled on the target system, in our case the ECDF cluster [36].

The direct integration of a one-loop matrix element over phase space with an adaptive Monte Carlo (MC) has two major disadvantages. The evaluation time of an NLO matrix element is considerable larger than that of a LO matrix element. Hence one should try to avoid unnecessary calls of the NLO matrix elements. The second problem are phase space regions where the chosen integral basis becomes linearly dependent and lead to numerical fluctuations. When these fluctuations reach the order of magnitude of the precision goal of the adaptive MC, the MC program tends to overestimate these phase space regions which can lead to numerical instabilities.

We avoid these problems by performing the phase space integration as a reweighting of unweighted LO Monte Carlo events. We use `WHIZARD` [4] an adaptive Monte Carlo integrator to obtain a list of unweighted LO events $\{p\}_i$ such that an observable O can be written as

$$\langle O \rangle_{\text{LO}} \equiv \int \mathrm{d}\Phi(\{p\}) |\mathcal{M}_{\text{LO}}|^2 O(\{p\}) = \lim_{N \to \infty} \frac{\sigma_{\text{LO}}}{N} \sum_{i=1}^{N} O(\{p\}_i) \qquad (2)$$

where the limit is understood in the statistical sense as a limit on the variance of the MC sum. The observable at one-loop precision is obtained as

$$\langle O \rangle_{\text{one-loop}} = \lim_{N \to \infty} \frac{\sigma_{\text{LO}}}{N} \sum_{i=1}^{N} K(\{p\}) O(\{p\}_i) \qquad (3)$$

with the local K-factor

$$K(\{p\}) = \frac{\mathcal{M}_{\mathrm{LO}}^{\dagger} \cdot (\mathcal{M}_{\mathrm{LO}} + \mathcal{M}_{\mathrm{virt}} + \mathbf{I} \cdot \mathcal{M}_{\mathrm{LO}})}{|\mathcal{M}_{\mathrm{LO}}|^2} \qquad (4)$$

The matrix elements $\mathcal{M}$ are understood as vectors in a given colour basis and $\mathbf{I}$ is the insertion operator as defined in [10], which ensures that after UV-renormalisation all poles in $1/(n-4)$ cancel. The reweighting can be understood as importance sampling with the probability density

$$w(\{p\}) \propto \frac{1}{\sigma_{\mathrm{LO}}} \frac{\mathrm{d}\sigma_{\mathrm{LO}}(\{p\})}{\mathrm{d}\Phi(\{p\})}. \qquad (5)$$

It should be emphasized that the definition of the local K-factor in Eq. (4) does not contain any real emission contributions and therefore the results below lack any physical interpretation.

3 Results for $u\bar{u} \to b\bar{b}b\bar{b}$

The results for the virtual correction of the process $u\bar{u} \to b\bar{b}b\bar{b}$ have been obtained with $n_f = 5$ massless quark flavours and for $p_T > 30\,\mathrm{GeV}$, a rapidity cut of $\eta < 2.5\,\mathrm{GeV}$ and a separation cut of $\Delta R = \sqrt{(\Delta\Phi)^2 + (\Delta\eta)^2} > 0.4$. The centre of mass energy is $14\,\mathrm{TeV}$. In this data set we choose the scales as $\mu_F = \mu_R = \sum_{i=1}^{4} p_{T,i}/4$ and fold with the CTEQ6.5 parton distribution functions [37]. We work with the modifications to the dipoles and insertion operators as proposed in [38]; for the distributions below we have evaluated the insertion operator at $\alpha_N = 0.1$. For this specific amplitude this modification induces a shift of the insertion operator of

$$\mathbf{I}_{\mathrm{unmodified}} - \mathbf{I}(\alpha_N) = \frac{\alpha_s(\mu)}{2\pi} \cdot 6\, C_F \left[\ln^2 \alpha_N - \frac{3}{2}(\alpha_N - 1 - \ln \alpha_N) \right]. \qquad (6)$$

On the ECDF cluster our code achieved a performance of $8.9\,\mathrm{s}$ ($17.6\,\mathrm{s}$) per phase space point and node[2] in double (quadruple) precision. The above timings suggest that an evaluation of the whole integration in quadruple precision is too costly to be practical and should be the last resort if double precision is not sufficient. The runtime will be improved further through code optimisations in the next version of the GOLEM code.

Figure 1 shows the distribution of the values for the local K-factor, the single pole and the double pole of an amplitude for 200,000 randomly chosen points in both double and quadruple precision. The distribution of the the K-factor shows that the values are sharply peaked around the the integrated result of $\mathcal{O}(1)$ and in double precision a small fraction of less than a percent of the points stretches out to atypically large values. It is clear that in a

---

[2]Xeon 5450 (quad-core), 3 GHz

data set of order 10^6 MC events a single outlier of that magnitude is already enough to tamper with the result. On the other hand, since the number of points in doubt is very small, an a posteriori test is enough and it suffices to re-evaluate those points at a higher precision. As possible test criteria we studied a cut on the K-factor, on the coefficient of the single pole and on the double pole; if the magnitude of the double precision result exceeds the cut the point is evaluated at higher precision.
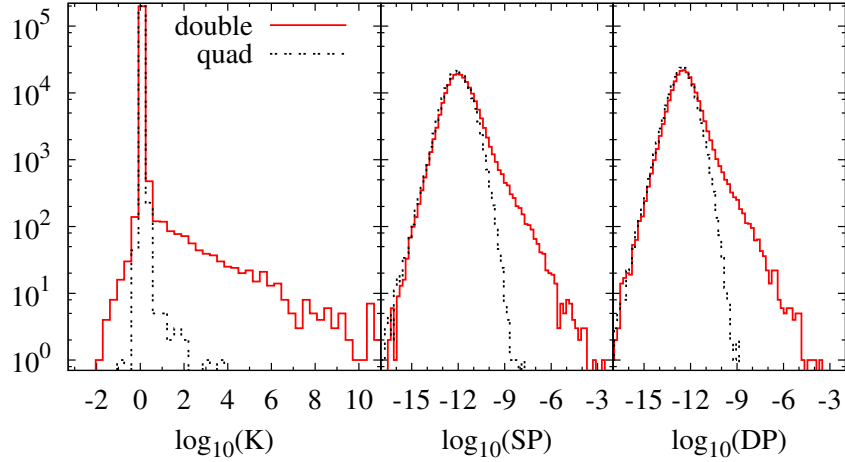
Figure 1: Comparison between evaluations of the matrix element for 200,000 MC events in double precision and quadruple precision. Shown are the distributions of the values of the local K-factor as defined in Eq. (4) (left) and the single $1/(n-4)$ (middle) and double $1/(n-4)^2$ (right) pole of the matrix element.

We have taken the same sample of 200,000 points to study the influence of the cut parameter on the integrated result. Figure 2 shows the relative error $\varepsilon_{\mathrm{rel}} = |\sigma(\mathrm{SP}_{\mathrm{cut}}) - \sigma(0)|/\sigma(0)$ on the cross-section versus the cut parameter $\mathrm{SP}_{\mathrm{cut}}$. The steep increase of the error indicates an outlier in the K-factor that is not reflected in the cancellation of the pole. A very similar picture emerges for a cut on the double pole (not shown). This lack of correlation between the pole cancellation and error on the integral can be circumvented by imposing a test on the local K-factor as shown in Figure 3. In the region between $2 \leq K_{\mathrm{cut}} \leq 5$ a relative error of $\approx 0.10\%$ is achieved while only 0.5% of the phase space points need to be evaluated at a higher precision.[3]

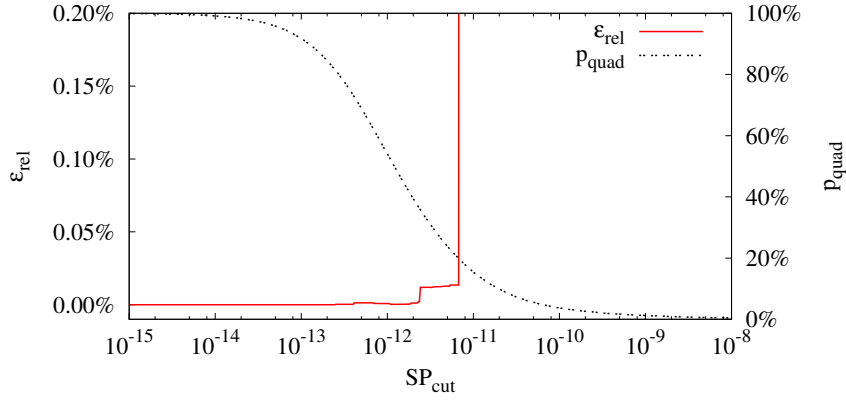[3]The downwards trend at $K_{\mathrm{cut}} \approx 10$ is a statistical fluctuation.

Figure 2: Relative error on the integrated result versus a cut SP_{cut} on the coefficient of the single pole. If the cancellation of the single pole in double precision is worse than SP_{cut} the data point is evaluated in quadruple precision. The dashed curve indicates the percentage of points that fail the test and need re-evaluation (right y-axis).
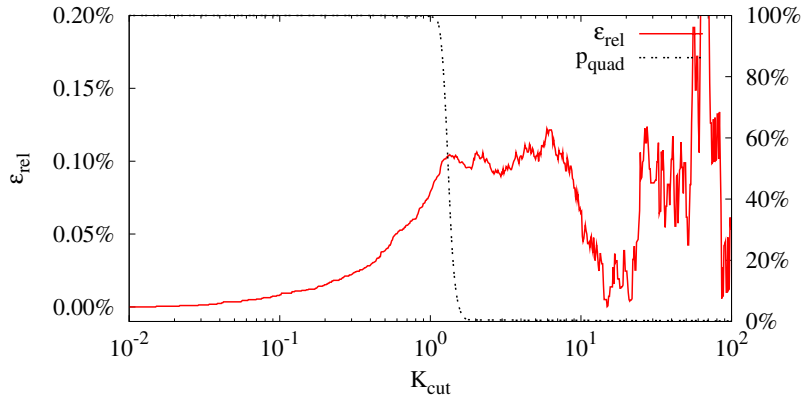

Figure 3: Relative error as in Figure 2 but with a cut on the local K-factor.
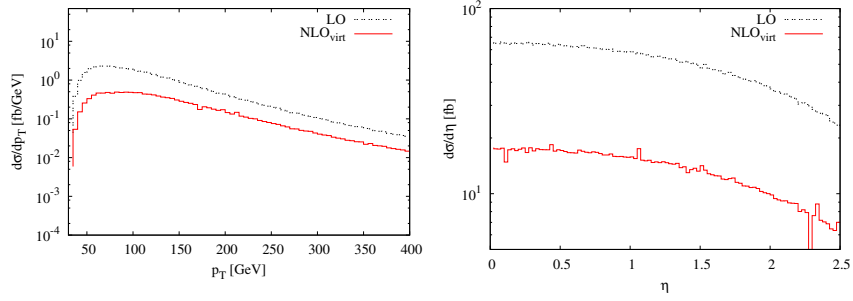
Figure 4: Distributions of the transverse momentum (left) and the rapidity (right) of the hardest jet. The result for $\mathrm{NLO_{virt}}$ is obtained from the finite contribution of the virtual part of the NLO prediction, as described in Eq. (4).
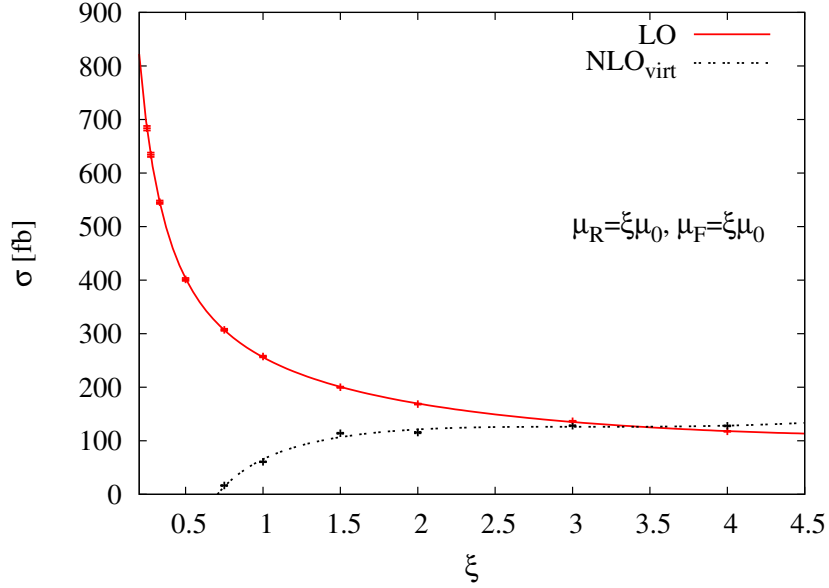

Figure 5: Stability under simultaneous variation of the renormalisation scale μ_R and the factorisation scale μ_F around the central value of $\mu_0 = \sum_{i=1}^{4} p_{T,i}/4$.

4   Conclusion

A successful interpretation of the LHC data will need precise predictions of both background and signal. For many processes this involves the evaluation of one-loop QCD amplitudes with many particles in the final state. We have presented the approach of the GOLEM collaboration to automatise such calculations that allows to generate code for the matrix element which is both fast and numerically stable in all relevant phase space regions. The need to control the accuracy of the result has been emphasised and a posteriori precision test has been proposed. We have introduced a new indirect integration method based on reweighting unweighted LO events by a local K-factor, which avoids certain problems that otherwise arise from a direct, adaptive MC integration of the one-loop matrix element. Results have been presented for the virtual corrections of the process $u\bar{u} \to b\bar{b}b\bar{b}$, which is part of an important background for MSSM Higgs boson searches at the LHC.

We have shown that our approach allows for efficient implementations for NLO predictions of processes with multi-particle final states and that the GOLEM project can lead to a fully automated tool for NLO calculations.

Acknowledgement

References

[1] ALEPH Collab., CDF Collab., D0 Collab., DELPHI Collab., L3 Collab., OPAL Collab., SLD Collab., LEP Electroweak Working Group, Tevatron Electroweak Working Group, SLD electroweak heavy flavour groups, "Precision Electroweak Measurements and Constraints on the Standard Model", arXiv:0811.4682 [hep-ex].

[2] "ATLAS detector and physics performance. Technical design report. Vol. 2",

[3] Z. Bern *et al.* [NLO Multileg Working Group], "The NLO multileg working group: summary report", arXiv:0803.0494 [hep-ph].

---

[4]http://www.edikt.org

[4] W. Kilian, T. Ohl and J. Reuter, "WHIZARD: Simulating Multi-Particle Processes at LHC and ILC", arXiv:0708.4233 [hep-ph].

[5] M. Moretti, T. Ohl and J. Reuter, "O'Mega: An optimizing matrix element generator", arXiv:hep-ph/0102195.

[6] F. Maltoni and T. Stelzer, "MadEvent: Automatic event generation with MadGraph", JHEP **0302** (2003) 027 [arXiv:hep-ph/0208156].

[7] F. Krauss, R. Kuhn and G. Soff, "AMEGIC++ 1.0: A matrix element generator in C++", JHEP **0202** (2002) 044 [arXiv:hep-ph/0109036].

[8] E. Boos *et al.* [CompHEP Collaboration], "CompHEP 4.4: Automatic computations from Lagrangians to events", Nucl. Instrum. Meth. A **534** (2004) 250 [arXiv:hep-ph/0403113].

[9] M. L. Mangano, M. Moretti, F. Piccinini, R. Pittau and A. D. Polosa, "ALPGEN, a generator for hard multiparton processes in hadronic collisions", JHEP **0307** (2003) 001 [arXiv:hep-ph/0206293].

[10] S. Catani and M. H. Seymour, "A general algorithm for calculating jet cross sections in NLO QCD", Nucl. Phys. B **485**, 291 (1997) [Erratum-ibid. B **510**, 503 (1998)] [arXiv:hep-ph/9605323].

[11] S. Catani, S. Dittmaier, M. H. Seymour and Z. Trocsanyi, "The dipole formalism for next-to-leading order QCD calculations with massive partons", Nucl. Phys. B **627**, 189 (2002) [arXiv:hep-ph/0201036].

[12] T. Gleisberg and F. Krauss, "Automating dipole subtraction for QCD NLO calculations", Eur. Phys. J. C **53** (2008) 501 [arXiv:0709.2881 [hep-ph]].

[13] M. H. Seymour and C. Tevlin, "TeVJet: A general framework for the calculation of jet observables in NLO QCD", arXiv:0803.2231 [hep-ph].

[14] K. Hasegawa, S. Moch and P. Uwer, "Automating dipole subtraction", Nucl. Phys. Proc. Suppl. **183**, 268 (2008) [arXiv:0807.3701 [hep-ph]].

[15] R. Frederix, T. Gehrmann and N. Greiner, "Automation of the Dipole Subtraction Method in MadGraph/MadEvent", JHEP **0809**, 122 (2008) [arXiv:0808.2128 [hep-ph]].

[16] C. F. Berger *et al.*, "An Automated Implementation of On-Shell Methods for One-Loop Amplitudes", 0803.4180 [hep-ph].

[17] S. Catani, T. Gleisberg, F. Krauss, G. Rodrigo and J. C. Winter, "From loops to trees by-passing Feynman's theorem", 0804.3170 [hep-ph].

[18] R. K. Ellis, K. Melnikov and G. Zanderighi, "Generalized unitarity at work: first NLO QCD results for hadronic W+3jet production", arXiv:0901.4101 [hep-ph].

[19] W. T. Giele and G. Zanderighi, "On the Numerical Evaluation of One-Loop Amplitudes: the Gluonic Case", 0805.2152 [hep-ph].

[20] R. K. Ellis, W. T. Giele, Z. Kunszt and K. Melnikov, "Masses, fermions and generalized D-dimensional unitarity", 0806.3467 [hep-ph].

[21] R. Britto, B. Feng and P. Mastrolia, "Closed-Form Decomposition of One-Loop Massive Amplitudes", 0803.1989 [hep-ph].

[22] G. Ossola, C. G. Papadopoulos and R. Pittau, "Reducing full one-loop amplitudes to scalar integrals at the integrand level", Nucl. Phys. B **763** (2007) 147 [hep-ph/0609007].

[23] A. Denner and S. Dittmaier, "Reduction schemes for one-loop tensor integrals", Nucl. Phys. B **734** (2006) 62 [hep-ph/0509141].

[24] Z. Bern, L. J. Dixon and D. A. Kosower, "On-Shell Methods in Perturbative QCD", Annals Phys. **322** (2007) 1587 [0704.2798 [hep-ph]].

[25] A. Bredenstein, A. Denner, S. Dittmaier and S. Pozzorini, "NLO QCD corrections to top anti-top bottom anti-bottom production at the LHC: 1. quark-antiquark annihilation", JHEP **0808** (2008) 108 [arXiv:0807.1248 [hep-ph]].

[26] T. Binoth *et al.*, "Precise predictions for LHC using a GOLEM", arXiv:0807.0605 [hep-ph].

[27] C. F. Berger *et al.*, "One-Loop Multi-Parton Amplitudes with a Vector Boson for the LHC", arXiv:0808.0941 [hep-ph].

[28] R. K. Ellis, W. T. Giele, Z. Kunszt, K. Melnikov and G. Zanderighi, "One-loop amplitudes for W+3 jet production in hadron collisions," JHEP **0901** (2009) 012 [arXiv:0810.2762 [hep-ph]].

[29] C. F. Berger *et al.*, "Precise Predictions for $W + 3$ Jet Production at Hadron Colliders", arXiv:0902.2760 [hep-ph].

[30] T. Reiter, "Automated Evaluation of One-Loop Six-Point Processes for the LHC", arXiv:0903.0947 [hep-ph].

[31] P. Nogueira, "Automatic Feynman graph generation", J. Comput. Phys. **105**, 279 (1993).

[32] T. Binoth, J. P. Guillet and G. Heinrich, "Reduction formalism for dimensionally regulated one-loop N-point integrals", Nucl. Phys. B **572** (2000) 361 [hep-ph/9911342].

[33] T. Binoth, J. P. Guillet, G. Heinrich, E. Pilon and C. Schubert, "An algebraic / numerical formalism for one-loop multi-leg amplitudes", JHEP **0510** (2005) 015 [hep-ph/0504267].

[34] J. A. M. Vermaseren, "New features of FORM", math-ph/0010025; J. A. M. Vermaseren and M. Tentyukov, "What is new in FORM", Nucl. Phys. Proc. Suppl. **160** (2006) 38.

[35] T. Binoth, J. P. Guillet, G. Heinrich, E. Pilon and T. Reiter, "Golem95: a numerical program to calculate one-loop tensor integrals with up to six external legs," arXiv:0810.0992 [hep-ph]. The code is available at http://lappweb.in2p3.fr/lapth/Golem/golem95.html.

[36] The Edinburgh Compute and Data Faclity (ECDF). http://www.ecdf.ed.ac.uk/.

[37] W. K. Tung, H. L. Lai, A. Belyaev, J. Pumplin, D. Stump and C. P. Yuan, "Heavy quark mass effects in deep inelastic scattering and global QCD analysis", JHEP **0702** (2007) 053 [arXiv:hep-ph/0611254].

[38] Z. Nagy, "Next-to-leading order calculation of three-jet observables in hadron-hadron collision", Phys. Rev. D **68** (2003) 094002 [arXiv:hep-ph/0307268].